JOURNAL OF PROPULSION AND POWER
Vol. 21, No. 2, March–April 2005

Design of a Near-Isentropic Supersonic Inlet Using Active Control

Umair Ahsun,* Ali Merchant,† James D. Paduano,† and Mark Drela‡
Massachusetts Institute of Technology, Cambridge, MA 02139

A two-dimensional Mach 2.2 internal compression inlet with 97% total pressure recovery has been designed using viscid–inviscid computational tools. Losses are minimized by careful boundary-layer management combined with shape design for weak shocks. The resulting inlet has reduced stability to unstart in the face of atmospheric and engine-borne disturbances, necessitating the use of an active stabilization bleed system that recovers the disturbance-rejection capabilities required of modern inlets. Atmospheric disturbances that the inlet may encounter during supersonic flight are characterized. Two separate physical mechanisms for unstart are identified, and active control algorithms to prevent these forms of unstart are designed and demonstrated using one- and two-dimensional unsteady Euler simulations. The resulting actively stabilized inlet can withstand flight velocity, temperature, and angle-of-attack perturbations consistent with atmospheric flight.

Introduction

AN inlet acts as an interface between the freestream and an aircraft propulsion system. The flow is decelerated to a Mach number required at the compressor face, and energy is recovered in the form of increased pressure. Although it is theoretically possible to design an inlet to achieve virtually isentropic compression of the supersonic flow to sonic conditions, in practice this may be impossible to realize due to flow disturbances and geometric variations in the inlet. Because shock waves contribute to loss in pressure recovery, a more realistic design is one that can achieve near-isentropic internal compression with a number of weak oblique shock waves and a weak terminal normal shock just behind the throat to decelerate the flow to subsonic conditions. Such a design is shown in Fig. 1.

The potential payoff of such a high-recovery inlet is significant. In the case of a typical 100,000-lb (45,300 kg) supersonic aircraft, such as the quiet supersonic platform, improving the inlet recovery to 97% in cruise could increase the range by approximately 500 n miles.[1] In addition, because most supersonic inlets require bleed on the order of 8% of the inlet flow to stabilize the terminal shock and control boundary-layer separation for the worst-case atmospheric disturbances, the reduced bleed requirement of the present design, primarily due to the weaker shock waves, may lead to additional gains at the system level.

The price of achieving high recovery is reduced stability to flow disturbances. These include atmospheric disturbances entering the inlet and engine-borne disturbances traveling upstream from the compressor face. These disturbances can cause a normal shock blowout event known as "inlet unstart."[2] Inlet unstart results in a severe increase in drag due to flow spillage and formation of a strong shock wave at the inlet lip. In addition, the accompanying decrease in mass flow through the inlet may also result in engine surge.

We can define the unstart tolerance of the inlet as the magnitude of the disturbance that can be tolerated without unstart. The tradeoff between inlet stability and pressure recovery is primarily a consequence of the strength of the terminal normal shock.[3] Thus, an inlet with a stronger normal shock, achieved by positioning the normal shock sufficiently downstream of the throat or alternatively by increasing the throat area ratio, will have a lower pressure recovery but will be more resistant to unstart under operational perturbations. Similarly, weakening the terminal normal shock will enhance the pressure recovery but will simultaneously make the terminal shock more susceptible to moving under operational perturbations, thus lowering the unstart tolerance of the inlet.

In this paper, the two-dimensional design and performance of an enhanced recovery inlet are presented. This is followed by a detailed discussion on the development of the active stabilization system for the inlet, which includes 1) characterizing and quantifying the atmospheric disturbances, 2) quantifying the dynamic behavior of the inlet subject to atmospheric disturbances for the design and analysis of a control system, and 3) development of the control architecture and control law. Finally, application of the active stabilization system illustrating its effectiveness in attenuating atmospheric disturbances is presented.

Design of Enhanced Recovery Inlet

A steady inviscid–viscous solver, based on the MISES solver approach, was used to design the two-dimensional profile and study the performance of the inlet.[4] The inviscid flow is represented by the axisymmetric Euler equations that are discretized on a streamline grid in a conservative form. The inviscid equations are strongly coupled with a two-equation integral boundary formulation via the displacement thickness concept. The fully coupled system of nonlinear equations is solved simultaneously by a global Newton–Raphson method. A boundary-layer suction model developed by Merchant was implemented in the code.[5] Comparison between the predictions of this suction model and experimental data has been carried out for a variety of subsonic and supersonic flows. The model assumes that the suction slot is flush with the inlet surface. Suction is applied by specifying a mass fraction, slot location, and slot width on the inlet geometry.

Inlet Design Approach

The primary consideration in the design of the inlet geometry is the pressure recovery. The losses that are considered in the present design are due to the oblique shock system in the supersonic portion of the inlet, the terminal normal shock, and the viscous boundary layers. The supersonic portion of the inlet can be made nearly isentropic at design conditions, which implies that the compression of the flow has to be gradual, and the length of the inlet cannot be overly constrained. On the other hand, because the inlet length has an impact on the viscous boundary-layer loss, a long inlet may not lead to the best recovery. A shorter inlet will also be lighter and preferable from the airframe–inlet integration point of view.

The critical Mach numbers in the inlet are at the throat, just upstream of the terminal normal shock, and at the exit (compressor

Presented as Paper 2003-4096 at the AIAA 16th Computational Fluid Dynamics Conference, Orlando, FL, 23–26 June 2003; received 31 January 2004; revision received 26 August 2004; accepted for publication 31 August 2004.

*Graduate Research Assistant, Department of Aeronautics and Astronautics.
†Research Engineer, Department of Aeronautics and Astronautics.
‡Associate Professor, Department of Aeronautics and Astronautics.

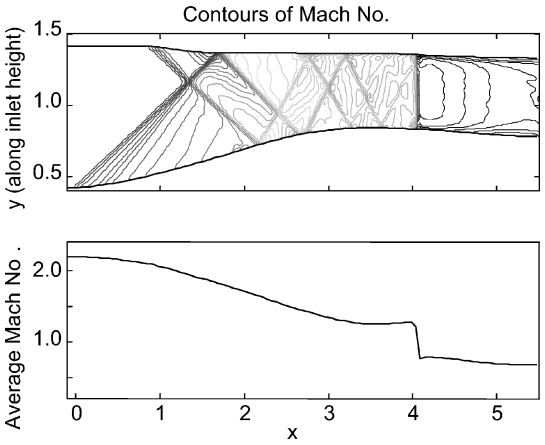

Fig. 1 Two-dimensional Euler calculation of a high-recovery internal compression inlet showing shock wave structure.

face). The normal shock Mach number contributes to the loss through the inviscid normal shock loss and through shock–boundary-layer interaction. The shock strength as well as inviscid shock loss increases rapidly for shock Mach numbers greater than about 1.3. The choice of shock Mach number constrains the throat Mach number such that

$$1 < M_{\text{throat}} < M_{\text{shock}} \tag{1}$$

Clearly, for stable operation, the throat Mach number must be greater than unity for supersonic inflow, and because supersonic flow must accelerate in a diverging duct to obey the area velocity relationship for an isentropic flow, the shock Mach number must be greater than the throat Mach number. The difference between M_{throat} and M_{shock} determines the range of inlet Mach-number variation that can be accepted by the inlet in the absence of control for stable operation and, therefore, affects the static stability of the inlet. From these considerations, a throat Mach number of 1.25 and shock Mach number of 1.27 were selected to meet the performance requirements while minimizing the bleed requirements.

Based on the inlet Mach numbers for current fan and compressor designs, which typically range from 0.5 to 0.65, an exit Mach number of 0.6 was chosen for the current design study. The inlet shape between the shock location and the exit plane was designed to achieve continuously decreasing pressure gradient to minimize the boundary-layer growth at the exit plane.

The two-dimensional profile of the inlet can be seen in Fig. 1. The length-to-height ratio of the inlet is 5.5. The ramp angle on the lower surface is 7 deg and the wedge angle on the upper surface is 4 deg. The upper surface is staggered with respect to the lower surface to cancel the compression waves emanating from these surfaces. The upper wedge angle was included in the design and calculations because the real inlet is expected to have some finite thickness, and a top-mounted configuration on the aircraft is expected.

Bleed Configuration

The inlet bleed configuration consists of a supersonic control bleed and two normal shock boundary-layer control bleeds. The steady value of the supersonic control bleed is 1% of the inlet mass flow, and it is modulated $\pm 1\%$ from its nominal value for active control. The bleed slot is positioned approximately one throat height upstream of the throat to meet the minimum time-delay requirements of the active control system. This position also coincides with the location where the oblique shock from the upper surface wedge impinges on the lower surface. This enables some degree of cancellation of the oblique shock reflection when the bleed is modulated. In addition to the supersonic bleed, two subsonic bleeds are located on the upper and lower surfaces just downstream of the normal shock location. The steady values of the lower and upper bleeds are 1 and 2% of the inlet mass flow. These bleeds serve a twofold purpose: 1) reducing the boundary-layer thickness critical for achieving the high pressure recovery and 2) stabilizing the shock in the face of incoming atmospheric and compressor face disturbances. The lower surface bleed is modulated $\pm 2\%$ from the nominal value for active control. The resulting total steady bleed requirement for the inlet is 4% of the inlet mass flow.

Atmospheric Disturbance Characterization

Although mechanisms such as aircraft maneuvers, backpressure perturbations due to engine transients, and so on can cause the inlet to unstart, atmospheric turbulence is the least predictable and, therefore, the most important factor in avoiding the inlet unstarts. To design an effective control system for the inlet, it is imperative to quantify the range and types of atmospheric disturbances encountered during nominal operation. The detailed derivations of the atmospheric disturbance models are discussed in Refs. 6 and 7.

During supersonic flight, the inlet may encounter velocity and temperature perturbations ranging from the macro scale (size greater than few hundred kilometers) through the mesoscale (from a few hundred to tens of kilometers) up to the micro scale (tens of kilometers to few centimeters). The scales imply a horizontal distance over which the disturbance parameter, such as the velocity, changes by its own order of magnitude. For the purpose of quantitatively expressing the disturbances, we can treat them as quasi-steady, which means, as the inlet is flying through the disturbances, they are stationary for an observer not moving with respect to the atmosphere. Using the stationary assumption, the atmospheric disturbances can be described statistically in terms of their power spectral density (PSD) functions. In the micro- and mesoscales the three-dimensional turbulence is isotropic, and we can use Kolmogorov's spectrum for turbulence as follows:

$$S_t(k) = \alpha_t \varepsilon^{\frac{2}{3}} k^{-\frac{5}{3}} \tag{2}$$

where the subscript t denotes a type of disturbance, ε is the eddy dissipation rate, k is the wave number, and α_t is a constant for each type of disturbance, given by $\alpha_l = 0.15$ (longitudinal or forward wind velocity gust, dimensionless), $\alpha_v = 0.2$ (vertical or upwind velocity gust, dimensionless), or $\alpha_T = 0.39$ (temperature disturbance, $\text{K}^2\text{s}^2\text{m}^{-2}$).

Data indicate that the $-\frac{5}{3}$ law spectral behavior just described extends uninterrupted to an outer scale disturbance wavelength of around 400 km.[6] Thus, we see that for a study of the effect of atmospheric disturbances on inlets only the eddy dissipation rate sets the spectral intensity over the entire frequency range of interest. The eddy dissipation rate is a function of the terrain, altitude, latitude, and time of year. A typical value for ε is 2.0×10^{-5} m^2s^{-3} and can vary as much as a factor of 10.

Using the given model spectra for different atmospheric disturbances, a Fourier series method can be used for the generation of a random time series that has the same spectra as the atmospheric disturbances.[8] A typical time domain output along with the relevant spectrum is shown in Fig. 2.

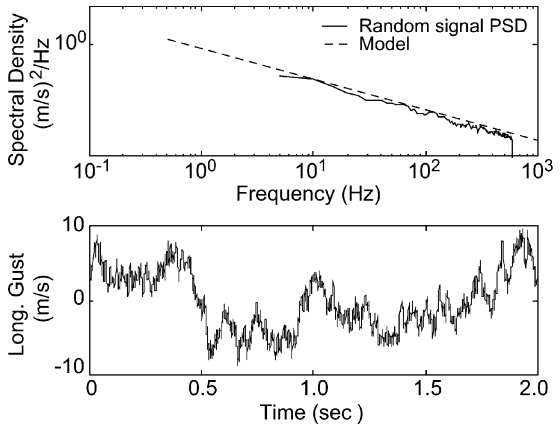

Fig. 2 Forward velocity gust time history and spectrum for an aircraft flying at Mach 2.2 at altitude of 60,000 ft (worst-case value of ε).

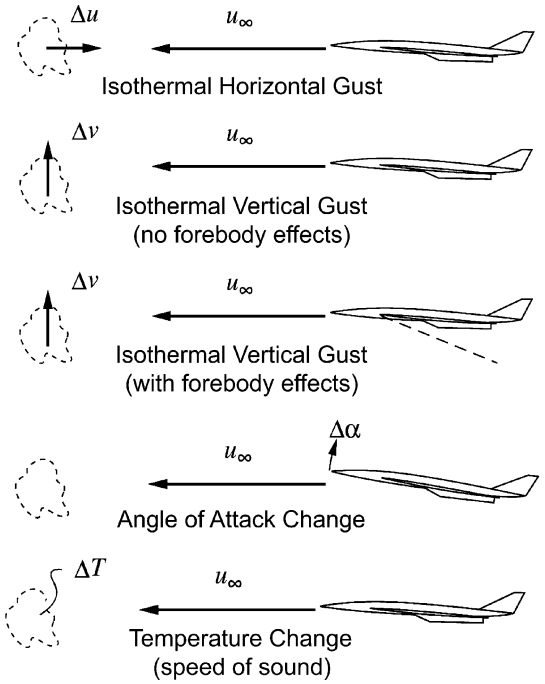

Fig. 3 Atmospheric disturbance components affecting the inlet during normal flight.

The atmospheric disturbances affecting the inlet can be characterized in terms of four independent components: isothermal longitudinal gust, isothermal vertical gust with and without a forebody, and temperature gust as shown in Fig. 3. Angle-of-attack changes can be expressed to first order in terms of the isothermal vertical gust. Also, for this study only the case with forebody is considered because it is relevant to the aircraft-inlet configuration of interest. These disturbance components are assumed to appear as plane waves at the inlet lip and to travel through the inlet in the form of characteristic waves. Using the linearized analysis for a quasi-one-dimensional flow through the inlet, these waves can be expressed as a superposition of fast acoustic waves J^+ traveling with a speed of $u + a$, slow acoustic waves J^- traveling with a speed of $u - a$, and entropy waves traveling with speed u. These variables are defined as follows:

$$J^+ = u + 2a/(\gamma - 1) \tag{3}$$

$$J^- = u - 2a/(\gamma - 1) \tag{4}$$

$$s = pv^\gamma \tag{5}$$

where u is local flow speed, a is the local speed of sound, s is the entropy, p is the pressure, v is the specific volume, and γ is the ratio of specific heats. The atmospheric disturbances are converted into the characteristic form, because the characteristic or "canonical" forms of the disturbances are directly applicable for the control law design.

Using the definition of characteristic variables and the Prandtl–Meyer wave relation for an isentropic flow turning through weak expansion/compression waves, we can write the transformation between the atmospheric variables and the canonical variables as

$$\begin{bmatrix} \Delta J+ \\ \Delta J- \\ \Delta s \end{bmatrix} = \begin{bmatrix} 1 & \dfrac{M_\infty - 1}{\sqrt{M_\infty^2 - 1}} & \dfrac{\gamma R}{(\gamma - 1)a_\infty} \\ 1 & -\dfrac{M_\infty + 1}{\sqrt{M_\infty^2 - 1}} & -\dfrac{\gamma R}{(\gamma - 1)a_\infty} \\ 0 & 0 & \dfrac{\gamma R}{\rho_\infty^{\gamma - 1}} \end{bmatrix} \begin{bmatrix} \Delta u \\ \Delta v \\ \Delta T \end{bmatrix} \tag{6}$$

where the right-hand-side vector represents the perturbations in forward velocity, vertical velocity, and temperature at the lip of the inlet. The transformation matrix shows an interesting relation: that a temperature perturbation impacts all the three canonical perturbations at the inlet lip.

Modification of Disturbance Spectra by Mach/Velocity Hold and Ramp Control

Atmospheric disturbances having very large wavelengths in the macroscale regions can exhibit large variations in gust velocities as discussed earlier. From the point of view of inlet control, we can assume that these large-scale disturbances (>6–20 km or frequencies below 0.03–0.1 Hz) will be absorbed by the aircraft velocity hold system. We can also envision a ramp-control system in the inlet that can modify the area properties of the inlet depending on the engine demand and atmospheric turbulence to avoid unstart. The inlet active control system will therefore be subject to the atmospheric disturbance spectra attenuated by the vehicle velocity hold system and the inlet ramp control system. Assuming a slew rate of approximately 60 deg/s for the ramp-control system and a cutoff frequency of around 0.33 rad/s for the Mach/velocity hold system, which is a typical value for supersonic aircraft in the same weight class, modified spectra can be obtained for the characteristic perturbations at the inlet lip.

The maximum frequency of interest for the inlet disturbance-rejection control system can be calculated from this modified spectrum. This is defined as the frequency that gives 99% of the spectral energy. For this particular spectrum, the maximum frequency is approximately 18 Hz. Thus, frequencies up to 18 Hz contribute 99% of the energy in the disturbance whereas higher frequencies only contribute the remaining 1%. From the point of view of the inlet control system, only frequencies up to 20 Hz are considered. On the lower side of the modified spectrum, we can see that frequencies below 0.01 Hz are cut off by the ramp-control and velocity hold systems. Thus, the range of frequencies of interest in the study of control system effectiveness is from 0.01 to 20 Hz for the full-scale aircraft. This results in nondimensional frequencies ranging from 4.4×10^{-5} to 0.1. The frequency is nondimensionalized by the inlet stagnation speed of sound and the inlet height at the forward lip.

It should be noted that the effective gain of the ramp and velocity/Mach hold systems is not infinity, and so for very low frequencies we may not get the rolloff at low frequencies. The atmospheric spectra also do not obey the $-\frac{5}{3}$ law for very low frequencies but instead overestimate the energy compared to the actual measurements of the disturbances.[7] Although a flattened spectrum is obtained at very low frequencies, we can safely assume that the disturbance energy is sufficiently attenuated at these low frequencies and has a negligible impact on the inlet stability.

Dynamic Characterization of the Inlet

The dynamic behavior of the inlet was analyzed using unsteady quasi-one- and two-dimensional inviscid numerical solvers. The solvers utilize a second-order accurate finite volume scheme for spatial discretization. Stabilization and shock capturing are enabled using Roe's scheme. A four-stage Runge–Kutta method is used to time march the solution. Boundary conditions are applied using Riemann invariants. The inlet boundary conditions were modified to impose the canonical atmospheric disturbances described earlier. The conservation laws were modified to include the effect of unsteady mass addition or removal in the simulation.

The unsteady numerical codes were embedded in Simulink and integrated into MATLAB to generate routines with the help of which different transfer functions could be generated to develop and analyze different control schemes. A block diagram of the Simulink model (called S-function) of the inlet is shown in Fig. 4. As shown in Fig. 4, the inlet can be excited with canonical atmospheric disturbances, characteristic disturbances, and bleed variations.

Frequency Response Study

Using the Simulink model, a detailed frequency response study was conducted for both quasi-one- and two-dimensional cases. The geometry used for the two-dimensional study was modified with a

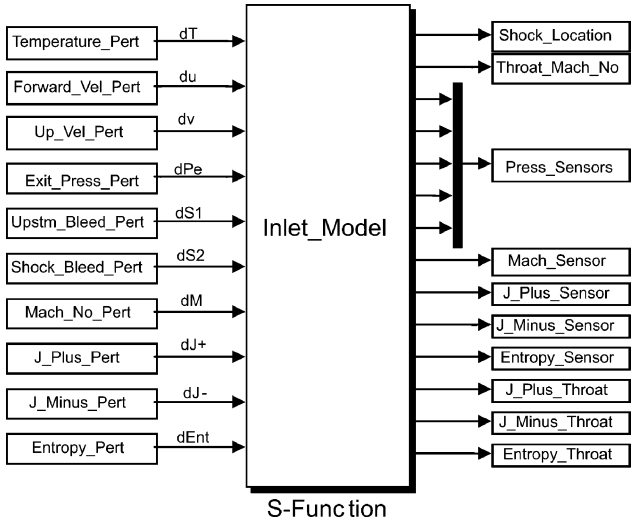

Fig. 4 Quasi-one-dimensional (and two-dimensional) unsteady Simulink model of the inlet.

viscous correction obtained from the steady viscous-inviscid design code described previously. The area variation for the quasi-one-dimensional study was created by matching the area ratio of the two-dimensional geometry at the inlet, the throat, and the exit. These critical areas were blended using cosine shape functions.

Figures 5a, 5b, and 5c present a comparison in the amplification of the characteristic disturbances for the quasi-one-dimensional and the area-averaged two-dimensional cases. This demonstrates that the quasi-one-dimensional model, especially in the low-frequency range, adequately represents the dynamic behavior of the inlet. Thus, for the purpose of designing the control laws for the inlet, we can utilize the quasi-one-dimensional unsteady model in the range of the frequencies of interest.

In Fig. 5a we can see that the effect of J^+ on the throat Mach number diminishes at higher frequencies. In contrast, Figs. 5b and 5c show that the effect of J^- remains essentially unchanged in the frequency range of interest, and the effect of entropy on the throat Mach number increases with frequency. The implication of these results is that J^- and entropy fluctuations have a greater impact than J^+ on the throat Mach number. Although the throat Mach-number amplification of J^+ and rolloff at higher frequency might suggest a negligible impact on unstart tolerance, J^+ has a significant impact on the shock motion. Figure 6 shows that the effect of bleed on the throat Mach number is essentially constant over the frequency range of interest. Though it is not apparent from the figure, the effect of bleed is primarily isentropic and is composed of J^+ and J^- perturbations as confirmed by simulations.

Normal shock motion as a function of different parameters has been studied via simplified linearized models that capture the shock dynamics with reasonable accuracy.[9] Analyzing the acoustic reflection and transmission properties of the normal shocks in ducts is crucial to understanding the shock motion.[10,11] MacMartin has derived an ordinary differential equation that captures the shock dynamics with reasonable accuracy.[12] The model shows that the transmission coefficient of upstream fast acoustic disturbances, or J^+, is nearly unity. Therefore, J^+ disturbances effectively pass through the shock with negligible effect on shock motion. However, from the large signal transfer function obtained in this study (Fig. 7a), we can see that the shock is strongly affected by the J^+ perturbations.

In comparison, the response of the shock motion to J^- and entropy perturbations, shown in Figs. 7b and 7c is substantially smaller. This can be explained in terms of the exit boundary condition used in the generation of the frequency response plots as follows. The inlet and compressor are coupled in a real operating environment and, to capture the detailed behavior of this inlet–engine interaction, an accurate compressor-face boundary condition (CFBC) has to be utilized. There have been a number of studies to create simplified models for the prediction of unsteady CFBC.[13,14] Sajben

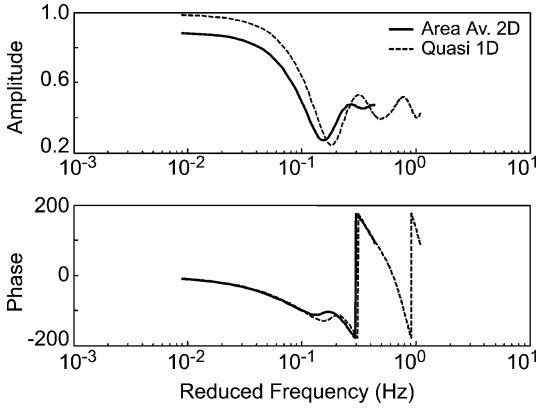

Fig. 5a Frequency response of the throat Mach number to fast acoustic wave (J^+) perturbations.

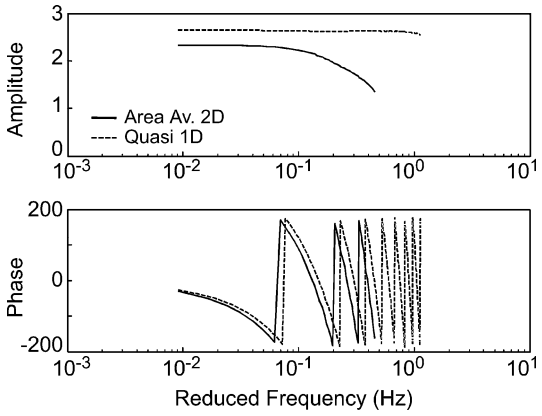

Fig. 5b Frequency response of the throat Mach number to slow acoustic wave (J^-) perturbations.

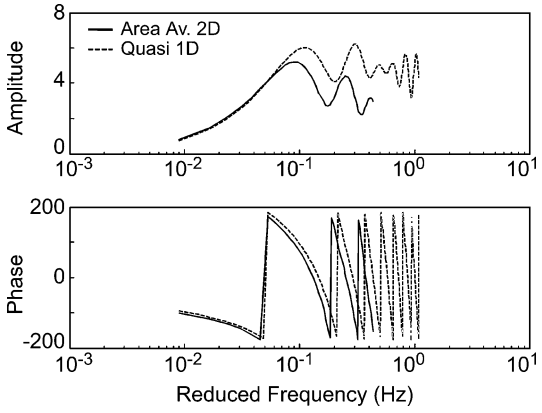

Fig. 5c Frequency response of the throat Mach number to entropy perturbations.

and Said have presented a simplified model for the computation of transmission and reflection coefficients accounting for compressor configuration and Mach number.[14] Their results show that for different compressor configurations and Mach numbers the reflection coefficient can vary widely, from −1 to 1. The constant exit pressure boundary condition used in the present study corresponds to the worst-case scenario of a reflection coefficient of −1. Because the transmission coefficient for the fast wave, J^+, through the shock is unity, the disturbance travels unattenuated to the exit boundary causing a reflection that has a strong effect on the shock position.

Bandwidth Requirements of the Actuator

An important parameter from the point of view of the control system design is the bandwidth requirements of the control system and actuator. It can be seen from the transfer function plots (Figs. 5a–5c)

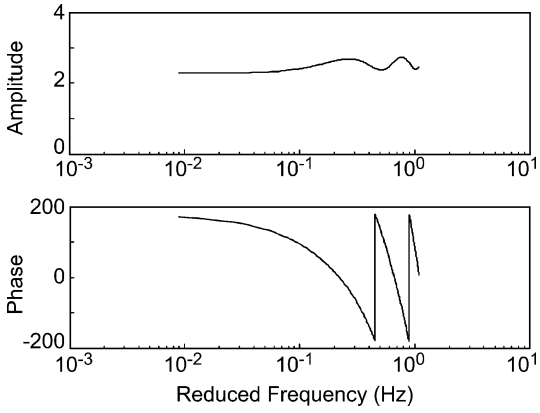

Fig. 6 Frequency response of the throat Mach number to upstream bleed perturbations.

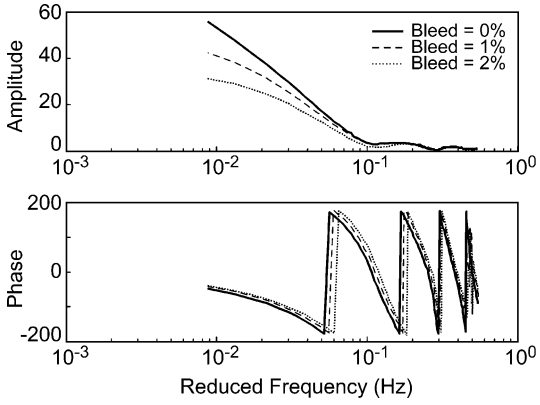

Fig. 7a Shock motion response (large signal) to fast acoustic wave (J^+) perturbations.

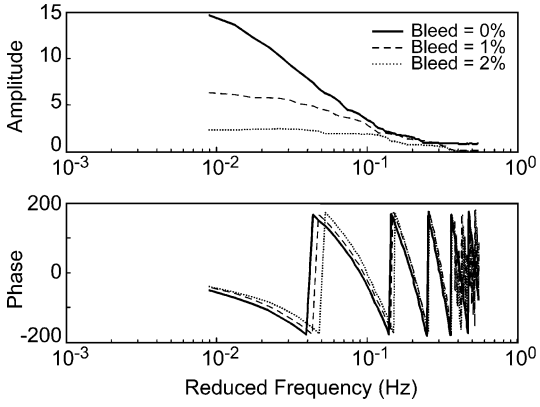

Fig. 7b Shock motion response (large signal) to slow acoustic wave (J^-) perturbations.

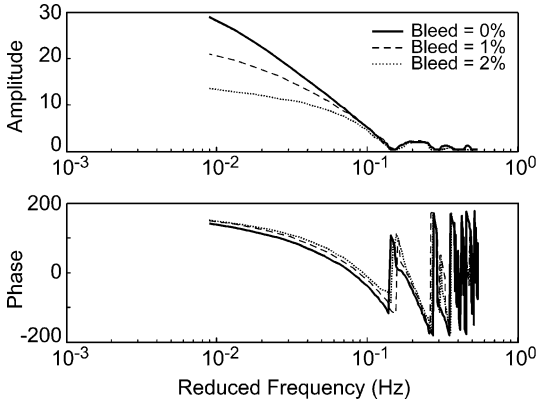

Fig. 7c Shock motion response (large signal) to entropy perturbations.

of the atmospheric disturbances that the inlet has a flat response over reduced frequencies up to 1 for slow waves. The inlet amplifies the entropy perturbations at higher frequencies. Thus, it is clear that the atmospheric perturbation cutoff, rather than the inlet itself, sets the bandwidth requirement. From the previous section it is clear that most of the atmospheric turbulence energy is concentrated at lower frequencies. This suggests that a dimensional frequency of around 20 Hz (corresponding to a nondimensional frequency of approximately 0.1) is the upper cutoff as far as the atmospheric perturbations are concerned. The bleed actuator must therefore have at least this bandwidth to cancel the effects of atmospheric perturbations.

Inlet Unstart Mechanisms

The inlet can unstart via two distinct mechanisms; 1) motion of the terminal normal shock from a stable position downstream of the throat to an unstable position upstream of the throat and 2) formation of a new unstable normal shock upstream of the throat.

The first mechanism is initiated by disturbances that directly affect the shock, such as reflection of fast waves from the exit boundary and entropy disturbances. Figures 7a and 7c illustrate the effect of these disturbances on the shock motion as described in the preceding section. The persistence of these disturbances over time can cause the shock to move upstream of the throat, leading to unstart. Such an event is shown in Fig. 8.

The second mechanism of unstart is caused by the strong impact of the slow acoustic wave disturbance J^- that has a much stronger effect on the throat Mach number compared to the shock motion itself. Thus, when a pulse of slow acoustic wave disturbance of a sufficient magnitude reaches the throat, it can unchoke the throat ($M_{\text{throat}} < 1$) while having virtually no impact on the stable normal shock downstream of the throat. Unchoking the throat therefore results in formation of an unstable shock downstream of the throat, leading to unstart. Figure 9 illustrates this unstart

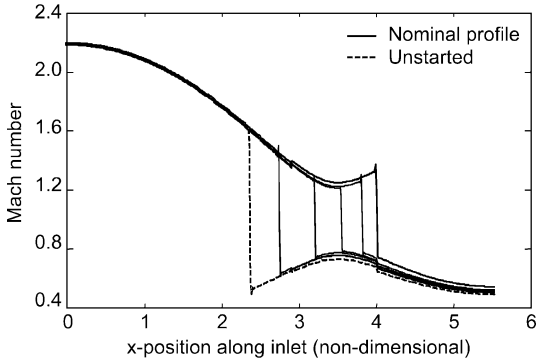

Fig. 8 Mach-number profiles for different normal shock locations: shock is moving toward the inlet lip due to an incoming atmospheric disturbance (unstart due to shock motion).

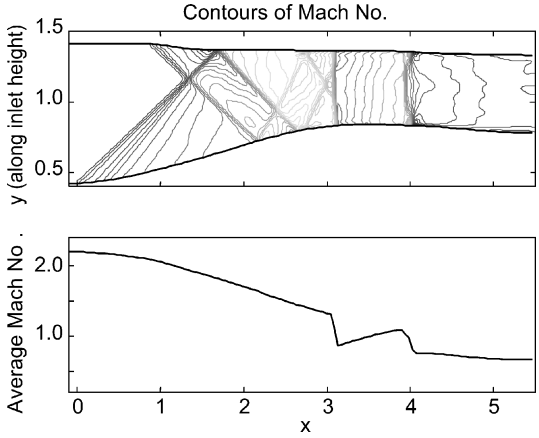

Fig. 9 Contours of Mach number for the unstarting inlet due to new shock formation at the throat.

mechanism. Formation of an unstable second normal shock is clearly seen in the Mach contours and the averaged-Mach-number profile.

Control Architecture

The dynamic response of the inlet shows that, in the range of the frequencies of interest, the quasi-one-dimensional and area-averaged two-dimensional transfer functions are almost identical and, in particular, the low-frequency response of the inlet is represented to a good approximation by quasi-one-dimensional simulation. Motivated by this observation, the control architecture design is based on the quasi-one-dimensional simulation results, because it is easier and simpler to design the control laws with the quasi-one-dimensional simulation and then test and verify the control laws in the two-dimensional simulation. The control laws are divided into two distinct parts to address the unstart mechanisms discussed in the preceding sections; namely, the throat Mach-number control and shock motion control.

Throat Mach-Number Control

The atmospheric disturbances can increase or decrease the throat Mach number significantly. Both the positive and negative variations are undesirable and must be controlled to enhance the stability of the inlet. The upstream bleed actuation is used to control the throat Mach number. Perturbations in the upstream bleed result in mostly slow acoustic waves as described previously, and from the speed of propagation of the slow acoustic waves we can estimate a time delay of approximately 2.0 nondimensional units for the control perturbations to reach the throat. This delay and the limited bandwidth of the actuator imply that we can only use a feedback control of the throat Mach number at very low frequencies. Therefore, to cover a wider range of frequencies in the incoming disturbance spectrum, we need to use a feedforward control system. The feedforward controller presented here is based directly on the atmospheric disturbance quantities, although the canonical disturbances, J^-, J^+, and entropy can also be used.

The longitudinal gust perturbation comprises both slow acoustic wave and fast acoustic wave perturbations. By using the longitudinal gust perturbations as our prime disturbance, we can cater for both J^+ and J^- perturbations. A static pressure sensor upstream of the bleed is used to estimate the Mach-number perturbations. The feedforward control architecture is shown in Fig. 10.

The change in throat Mach number due to upstream longitudinal gust perturbation $\mathrm{d}u$ and upstream bleed perturbation $\mathrm{d}s1$ are given as

$$\mathrm{d}M_{\mathrm{th}} = G_{M\mathrm{th}\_du}(j\omega)\,\mathrm{d}u + G_{M\mathrm{th}\_ds1}(j\omega)\,\mathrm{d}s1 \tag{7}$$

where $G_{M\mathrm{th}\_du}(\mathrm{j}\omega)$ is the transfer function (TF) from longitudinal gust at the inlet lip to the throat Mach number while $G_{M\mathrm{th}\_ds1}(\mathrm{j}\omega)$ is the TF from upstream bleed to the throat Mach number (shown in Fig. 6).

Using the controller gain $K(j\omega)$ we can express Eq. (7) as

$$\mathrm{d}M_{\mathrm{th}} = G_{M\mathrm{th}\_du}(j\omega)\,\mathrm{d}u + G_{M\mathrm{th}\_ds1}(j\omega)K(j\omega)G_{Ms\_du}(j\omega)\,\mathrm{d}u \tag{8}$$

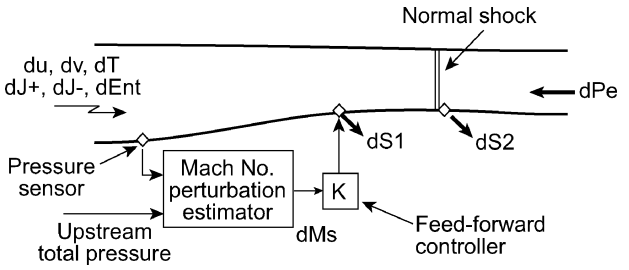

Fig. 10 Feedforward control law architecture, for throat Mach-number control, based on Mach-number estimation at the sensor.

The controller gain $K(j\omega)$ for cancellation of the throat Mach-number perturbation is

$$K(j\omega) = -\left[\frac{G_{M\mathrm{th}\_du}(j\omega)}{G_{M\mathrm{th}\_ds1}(j\omega)G_{Ms\_du}(j\omega)}\right]_{\text{Stable, Realizable Part}} \tag{9}$$

A typical controller frequency response and its synthesis using infinite impulse response (IIR) filter is shown in Fig. 11.

Shock Motion Control

Shock motion can be controlled by sensing the location of the shock by an array of static pressure sensors.[15] Using the location of the shock as feedback, a simple proportional controller can be used to drive the shock bleed to keep the shock stable in the face of compressor and atmospheric disturbances as shown in Fig. 12.

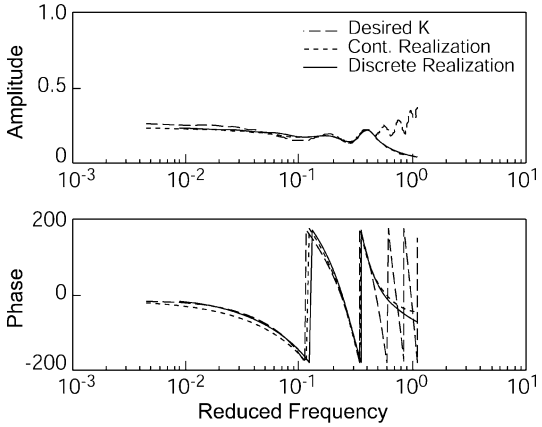

Fig. 11 Frequency response of the feedforward controller and its realizations.

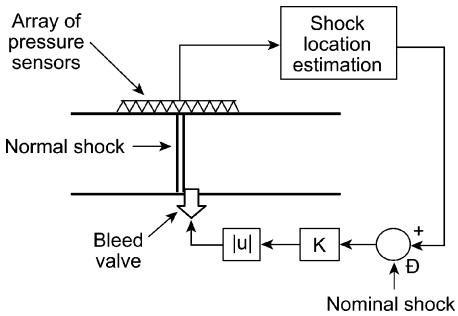

Fig. 12 Shock position control using shock location feedback.

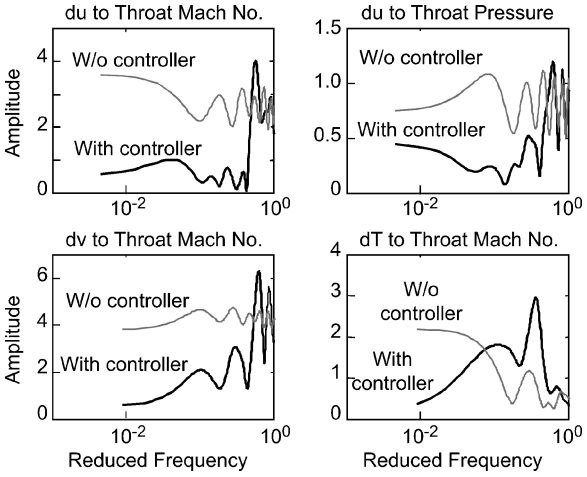

Fig. 13 Controller effectiveness for changes in throat Mach number and pressure.

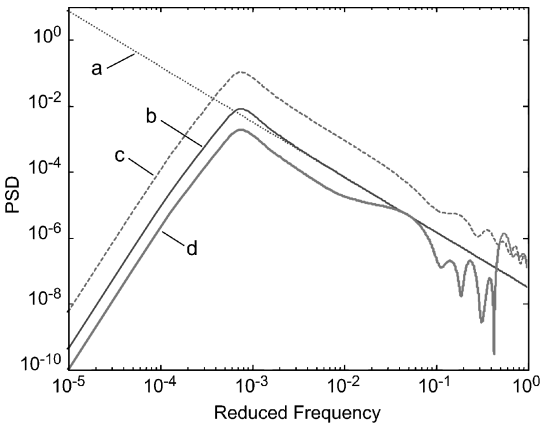

Fig. 14a PSD of throat Mach-number variations with and without forward velocity gust control: a) original PSD (forward velocity), b) with ramp and velocity hold, c) throat Mach No. variations without control, and d) throat Mach No. variations with control.

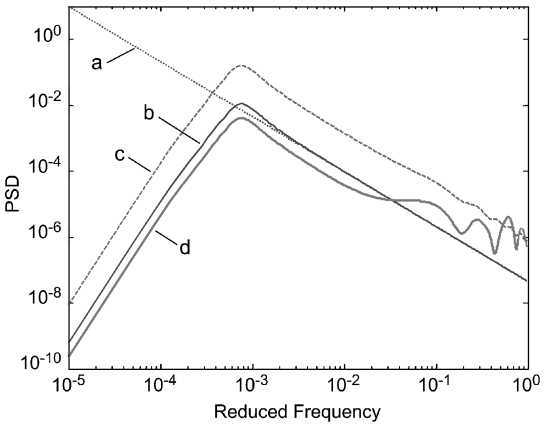

Fig. 14b PSD of throat Mach-number variations with and without vertical velocity gust control: a) original PSD (vertical velocity), b) with ramp and velocity hold, c) throat Mach No. variations without control, and d) throat Mach No. variations with control.

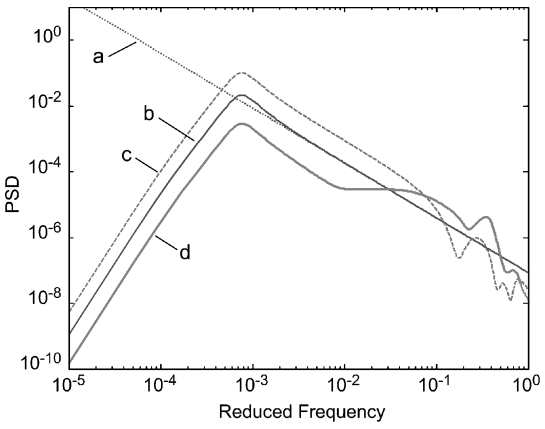

Fig. 14c PSD of throat Mach-number variations with and without temperature gust control: a) original PSD (temperature gust), b) with ramp and velocity hold, c) throat Mach No. variations without control, and d) throat Mach No. variations with control.

A detailed discussion of shock motion control using this technique can be found in Ref. 12.

Results

The aforementioned control architecture was tested in the two-dimensional unsteady simulation embedded in Simulink. Figure 13 shows the impact of the controller in attenuating the longitudinal (forward) gust, vertical gust, and temperature perturbations. Whereas the temperature perturbations were neglected in the design of the feedforward controller, Fig. 13 shows that, over most of the low-frequency range of interest, the controller is able to cancel the temperature perturbations.

Table 1 RMS value of throat Mach-number variations with control and without control

Disturbance type	RMS M_{throat} w/o control ($\times 10^{-3}$)	RMS M_{throat} with control ($\times 10^{-3}$)
Horizontal gust	11.0	1.7
Vertical gust	13.8	2.7
Temperature	10.8	2.6
J^+	16.2	5.2
J^-	48.3	6.4
Entropy	8.7	9.7

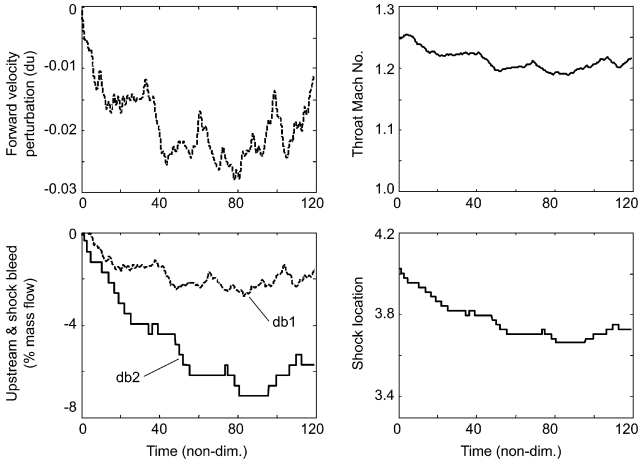

Fig. 15 Time response, using two-dimensional simulation, of the inlet to a typical atmospheric gust in forward velocity; note that area-averaged values of the variables are shown.

The controller effectiveness can also be examined via the spectrum of the atmospheric disturbances at the throat. Figures 14a–14c show the spectrum of the atmospheric disturbances and variations in throat Mach number with and without control. Figure 14c shows that, while temperature disturbances above the maximum frequency of interest (0.1) are amplified, the controller is still effective for lower frequency disturbances where the maximum energy is concentrated. Table 1 shows the rms values of the throat Mach-number variations due to different types of disturbances. A substantial reduction in the rms values of the throat Mach number for the various disturbances is achieved with active control.

It is also apparent that this control architecture is most effective in attenuating slow acoustic waves, and entropy perturbations are mildly amplified by the controller. This is expected because the bleed cancels the slow acoustic perturbations more effectively than the fast acoustic and entropy perturbations.

Figure 15 shows a time-domain result from two-dimensional simulation for a typical gust in forward velocity. In this simulation result both the upstream and downstream controllers were on and they were able to stabilize the shock and prevented unstart.

Conclusions

The design of a high-recovery inlet with reduced stability to unstart has been presented. Enhanced recovery can have a substantial impact on propulsion systems for long-range supersonic aircraft. The atmospheric turbulence is studied and characterized to develop suitable control laws for the inlet. The dynamic characteristics of the inlet are modeled using quasi-one-dimensional and two-dimensional Euler equations. The quasi-one-dimensional simulation of the inlet dynamics, which was shown to be in good agreement with the two-dimensional simulation in the range of the frequencies of interest, was used to develop the control algorithm. The stability of the inlet was enhanced using a simple feedforward controller that significantly reduced the rms values of the throat Mach-number perturbations to various incoming disturbance types.

Using separate estimators for the slow and fast waves, and designing a controller to cancel these waves, can improve the performance of the present throat Mach-number controller.

Acknowledgments

Research presented in this paper was funded by the Defense Advanced Research Projects Agency under the micro adaptive flow control (MAFC) program. The authors thank the members of the actively stabilized isentropic supersonic inlet (ASISI) group at the Massachusetts Institute of Technology Gas Turbine Laboratory for their contributions to this work.

References

[1]Paduano, J., Merchant, A., Drela, M., Lassaux, G., and Schuler, B., "Design and Testing of a High-Recovery, Actively Controlled Supersonic Inlet," Gas Turbine Lab., Massachusetts Institute of Technology, MIT GTL Rept., Cambridge, MA, Jan. 2002.

[2]Mayer, D. W., and Paynter, G. C., "Prediction of Supersonic Inlet Unstart Caused by Freestream Disturbances," *AIAA Journal*, Vol. 33, No. 2, 1995.

[3]Soreide, D., Bogue, R., Seidel, J., and Ehernberger, L. J., "The Use of a LIDAR Forward-Looking Turbulence Sensor for Mixed-Compression Inlet Unstart Avoidance and Gross Weight Reduction on a High Speed Civil Transport," AIAA Paper 97-3035, July 1997.

[4]Youngren, H., and Drela, M., "Viscous/Inviscid Method for Preliminary Design of Transonic Cascades," AIAA Paper 91-2364, June 1991.

[5]Merchant, A., and Drela, M., "Design and Analysis of Supercritical Airfoils with Boundary Layer Suction," AIAA Paper 96-2397, June 1996.

[6]Tank, W. G., and Gillis, J., "Atmospheric Disturbance Models for Linear and Nonlinear System Response Analysis," AIAA Paper 96-0394, Jan. 1996.

[7]Tank, W. G., "Atmospheric Disturbance Environment Definition," NASA CR-195315, Feb. 1994.

[8]Fairall, C. W., and White, A. B., "A Stochastic Model of Gravity-Wave Induced Clear Air Turbulence," *Journal of Atmospheric Sciences*, Vol. 49, Aug. 1991, pp. 1771–1790.

[9]Hurrell, H. G., "Analysis of Shock Motion in Ducts During Disturbances in Downstream Pressure," NACA TN 4090, 1957.

[10]Culick, F. E. C., and Rogers, T., "The Response of Normal Shocks in Diffusers," *AIAA Journal*, Vol. 21, No. 10, 1983, pp. 1382–1390.

[11]Yang, V., and Culick, F. E. C., "Analysis of Unsteady Inviscid Diffuser Flow with a Shock Wave," *Journal of Propulsion and Power*, Vol. 1, No. 3, 1985, pp. 222–228.

[12]MacMartin, D. G., "Dynamics and Control of Shock Motion in a Near-Isentropic Inlet," *Journal of Aircraft*, Vol. 41, No. 4, 2004, pp. 846–853.

[13]Freund, D., and Sajben, M., "Experimental Investigation of Outflow Boundary Conditions Used in Unsteady Inlet Flow Computation," AIAA Paper 97-0610, Jan. 1997.

[14]Sajben, M., and Said, H., "Acoustic-Wave/Blade-Row Interactions Establish Boundary Conditions for Unsteady Inlet Flows," *Journal of Propulsion and Power*, Vol. 17, No. 5, 2001, pp. 1096, 1097.

[15]Sajben, M., Donovan, J. F., and Morris, M., "Experimental Investigation of Terminal Shock Sensors for Mixed-Compression Inlets." *Journal of Propulsion and Power*, Vol. 8, No. 1, 1992, pp. 168–174.